

A partitioned solution procedure for simulating water flow in a variably saturated dual-porosity medium

Peng-Hsiang Tseng,* Antonella Sciortino & M. Th. van Genuchten

US Salinity Laboratory, 450 Big Springs Road, USDA, ARS, Riverside, California 92507, USA

(Received 7 November 1994; accepted 19 June 1995)

A simple and computationally effective partitioned solution procedure was used to solve the coupled equations of water flow in a variably-saturated dual-porosity medium. The coupled equations were first discretized in space and time using standard numerical solution procedures. The resulting algebraic system was subsequently partitioned in the time domain with a staggered implicit-implicit partitioning scheme. The partitioned time-integration procedures were carried out sequentially for the two subsystems, and coupled by temporal extrapolation techniques. A numerical stability and accuracy analysis demonstrated that the partitioned solution scheme, when integrated with the midpoint rule, is unconditionally stable and second-order accurate with only a single-pass through the partitioned equations (i.e. without iteration between the two subsystems). Simulation examples revealed that the solution of the single-pass scheme yields a slightly delayed response to that of the iterative scheme.

Key words: unsaturated flow, dual-porosity model, structured porous media, partitioned solution method.

INTRODUCTION

Dual-porosity models have been extended and used, with various simplifying assumptions, to simulate water flow and solute transport in structured, variably-saturated porous media ever since Barenblatt and Zheltov¹ and Barenblatt *et al.*² first introduced a conceptual double-continua approach in 1960 for water flow in fissured groundwater systems. The dual-porosity model approximates the physical system of a structured medium with two distinct, but interacting, subsystems which represent macropores and porous blocks inherent in field soil or rock formations. Equations which govern water flow and/or solute transport are described separately for each subsystem and suitably coupled to account for the exchange of fluid and/or contaminants between the two interacting continua. A comprehensive review of related modeling approaches was given by Mills *et al.*¹³

In order to simulate the preferential flow of water

under variably saturated conditions, Gerke and van Genuchten⁸ recently suggested using a set of coupled Richards equations describing transient water flow in each of the two subsystems. The exchange of fluid between the two subsystems was approximated by a first-order nonlinear transfer term. While such an integrated approach appears promising in understanding the underlying processes operative in a complex physical system, one major difficulty in using the model as a practical tool in research or application involves the development of accurate and computationally efficient numerical solution schemes.⁸

As an alternative to the simultaneous solution procedure used by Gerke and van Genuchten,⁸ we studied the possibility of using a partitioned solution approach for solving the coupled set of equations. Such an approach has been shown^{6,16} to have certain advantages in terms of program modularity and computational efficiency. Unfortunately, the partitioning method for certain applications may suffer from a numerical stability restriction, especially when the increased computational efficiency is achieved in an *ad hoc* fashion.¹⁶ In order to achieve minimal computational effort while maintaining satisfactory numerical stability and accuracy, several

*Present address: Institute of Geophysics and Planetary Physics, University of California, Riverside, California 92521, USA.

investigators successfully applied a judiciously chosen predictor combined with a matrix augmentation technique or other suitable modification to a variety of coupled problems.^{5,12,15,17,19,21} Still, the issue of developing a suitable partitioning algorithm for a particular coupled problem of interest remains a challenge.

The objective of this study is to develop a numerical solution method suitable for practical application of water flow in a variably saturated dual-porosity medium. A computationally efficient partitioned solution procedure is presented for this purpose. The numerical stability and accuracy of the solution procedure is analyzed in detail. Two simulation examples are presented to illustrate the performance of the partitioned scheme under various conditions. Underlying conceptual issues are not further addressed in this paper since they have been discussed at length by Gerke and van Genuchten.^{8,9}

GOVERNING EQUATIONS

The governing equations for one-dimensional Darcian water flow in a variably saturated rigid dual-porosity medium, under the assumptions that the pressure is constant in the air phase and the fluid is incompressible, are taken as⁸

$$C_f \frac{\partial h_f}{\partial t} = \frac{\partial}{\partial x} \left(K_f \frac{\partial h_f}{\partial x} - K_f \cos \alpha \right) - \frac{\Gamma_w}{\epsilon_f} - S_f \quad (1a)$$

$$C_m \frac{\partial h_m}{\partial t} = \frac{\partial}{\partial x} \left(K_m \frac{\partial h_m}{\partial x} - K_m \cos \alpha \right) + \frac{\Gamma_w}{1 - \epsilon_f} - S_m \quad (1b)$$

where the subscripts f and m denote the subsystems of fractures (macropores) and matrix blocks (micropores), respectively; $C = \partial \theta / \partial h$ is the specific soil-water capacity, θ is the volumetric water content, h is the soil-water pressure head, K is the hydraulic conductivity, ϵ is a volume fraction, S is a sink term, Γ_w is the mass exchange term for water, t is time, x is the spatial coordinate, and α is the angle between the vertical z -axis (positive downward from the soil surface) and the water flow direction, x , measured from z to x and defined positive counterclockwise.

The water exchange term, Γ_w , between the two subsystems is assumed to be⁸

$$\Gamma_w = \alpha_w (h_f - h_m) \quad (2)$$

where α_w is a first-order mass transfer coefficient for water as follows

$$\alpha_w = \frac{\beta}{a^2} \gamma_w K_a \quad (3)$$

where β is a coefficient related to the geometry of the

matrix blocks, a is the characteristic half-width of the matrix block, K_a is the apparent hydraulic conductivity at the interface of the two subsystems, and γ_w is an empirical coefficient. A detailed discussion of eqns (2) and (3) is given by Gerke and van Genuchten.⁹

The water retention and hydraulic conductivity properties of both subsystems are assumed to be given by the expressions²⁰

$$\theta(h) = \theta_r + \frac{\theta_s - \theta_r}{(1 + |\alpha h|^n)^m} \quad h < 0 \quad (4a)$$

$$\theta(h) = \theta_s \quad h \geq 0$$

$$K(h) = K_s K_r(h) \quad h < 0 \quad (4b)$$

$$K(h) = K_s \quad h \geq 0$$

respectively, where

$$K_r = S_e^{1/2} [1 - (1 - S_e^{1/m})^m]^2 \quad (4c)$$

$$S_e = (\theta - \theta_r) / (\theta_s - \theta_r)$$

and where θ_s and θ_r denote the saturated and residual volumetric water content, respectively; K_s and K_r are the saturated and relative hydraulic conductivity, respectively; S_e is effective saturation, α , m , and n are constant shape parameters, and $m = 1 - 1/n$.

NUMERICAL SOLUTION PROCEDURES

The partitioned procedure permits one, at least in practice, to apply different spatial discretization and time integration schemes for each subsystem depending upon the characteristics of the physical system. However, our analysis below assumed that the two subsystems are discretized with identical grids in space and integrated with the same numerical scheme in time. Partitioned methods for coupled systems can be formulated on two different partitioning levels, i.e. differential and algebraic partitioning. Previous studies (e.g. Park & Felippa¹⁶) suggest that algebraic partitioning has better implementation flexibility. For algebraic partitioning, eqns (1a) and (1b) were first semi-discretized in space using standard Galerkin procedures; this resulted in a set of first-order coupled ordinary differential equations in time of the form

$$\begin{bmatrix} \mathbf{C}_f & 0 \\ 0 & \mathbf{C}_m \end{bmatrix} \begin{Bmatrix} \dot{\mathbf{h}}_f \\ \dot{\mathbf{h}}_m \end{Bmatrix} + \begin{bmatrix} \mathbf{K}_f + \mathbf{E} & -\mathbf{E} \\ -\mathbf{E} & \mathbf{K}_m + \mathbf{E} \end{bmatrix} \begin{Bmatrix} \mathbf{h}_f \\ \mathbf{h}_m \end{Bmatrix} = \begin{Bmatrix} \mathbf{f}_f(t) \\ \mathbf{f}_m(t) \end{Bmatrix} \quad (5)$$

in which \mathbf{h} is the discrete pressure head vector, \mathbf{C} and \mathbf{K} are the capacity (or mass) and conductivity (or stiffness) matrices, respectively, \mathbf{E} is the interaction matrix which contains the coupling term between the two subsystems, and \mathbf{f} is a vector of forcing functions which includes

information from boundary conditions and source/sink terms. The superscript dot denotes temporal differentiation. Matrix \mathbf{C} is always symmetric and positive definite. Matrices \mathbf{K} and \mathbf{E} are also symmetric and may be specified as positive definite or positive semi-definite depending upon the problem being considered. Detailed expressions for the above matrices are given in the Appendix. Note that the matrices \mathbf{C} , \mathbf{K} , and \mathbf{E} are functions of the corresponding state variable \mathbf{h} .

One important feature of time integration for each subsystem in (5) is the possibility of mass balance errors often encountered in traditional finite element formulations. Mass conservative schemes for the mixed and h -based forms of the Richards equation have been suggested by Celia *et al.*⁴ and Rathfelder and Abriola,¹⁸ respectively. For both approaches, caution was taken to formulate the discretized form of the storage term equivalent to its continuous differential counterpart. Another important consideration of numerical approximation is the stability behaviour of the applied algorithm. Gourlay¹⁰ and Hughes¹¹ demonstrated that the commonly used one-step second-order accurate trapezoidal rule (or Crank–Nicolson method) is unconditionally stable only for linear parabolic systems, but not for nonlinear formulations such as is the case when the Richards equation is used. These same two authors^{10,11} suggested a midpoint rule which possesses stability properties that are the same for both linear and nonlinear cases.

Application of a generalized midpoint rule to each subsystem of eqn (5), and evaluating the capacity coefficients by the standard chord-slope approximation,¹⁸ yields

$$\mathbf{H}\mathbf{x}^{n+1} = \mathbf{g} \quad (6a)$$

where

$$\begin{aligned} \mathbf{H} &= \mathbf{A}^{n+\alpha} + \alpha\Delta t\mathbf{B}^{n+\alpha} \\ \mathbf{g} &= \Delta t\mathbf{d}^{n+\alpha} + [\mathbf{A}^{n+\alpha} - (1-\alpha)\Delta t\mathbf{B}^{n+\alpha}]\mathbf{x}^n \\ \mathbf{x}^T &= [\mathbf{h}_f \ \mathbf{h}_m] \quad \mathbf{d}^T = [\mathbf{f}_f \ \mathbf{f}_m] \end{aligned} \quad (6b)$$

$$\mathbf{A} = \begin{bmatrix} \mathbf{C}_f & 0 \\ 0 & \mathbf{C}_m \end{bmatrix} \quad \mathbf{B} = \begin{bmatrix} \mathbf{K}_f + \mathbf{E} & -\mathbf{E} \\ -\mathbf{E} & \mathbf{K}_m + \mathbf{E} \end{bmatrix}$$

in which the superscript n denotes the time level, $\Delta t = t^{n+1} - t^n$ is the time step increment, α is a dimensionless time weighting factor, and \mathbf{x}^T and \mathbf{d}^T are the transpose of \mathbf{x} and \mathbf{d} , respectively. The right-hand side vector, \mathbf{g} , contains previously computed solutions only, and hence is often referred to as the historical term. Note that for the midpoint rule, all time-dependent parameters of a subsystem are evaluated at the same time level. The resulting time-discrete coupled set of algebraic system (6) is partitioned in accordance with problem characteristics.

Various partitioning techniques were discussed in detail by Park and Felippa.¹⁶ An appropriate partitioning scheme for the dual-porosity model is staggered implicit–implicit partition. This approach partitions the matrix \mathbf{B} into an implicit part \mathbf{B}_I and an explicit part \mathbf{B}_E as

$$\mathbf{B} = \mathbf{B}_I + \mathbf{B}_E = \begin{bmatrix} \mathbf{K}_f + \mathbf{E} & 0 \\ -\mathbf{E} & \mathbf{K}_m + \mathbf{E} \end{bmatrix} + \begin{bmatrix} 0 & -\mathbf{E} \\ 0 & 0 \end{bmatrix} \quad (7)$$

Transferring the explicit part \mathbf{B}_E to the right-hand side of (6a) yields

$$\mathbf{H}_I\mathbf{x}^{n+1} = \mathbf{g} - \alpha\Delta t\mathbf{B}_E^{n+\alpha}\mathbf{x}^{n+1^p} \quad (8a)$$

where

$$\mathbf{H}_I = \mathbf{A}^{n+\alpha} + \alpha\Delta t\mathbf{B}_I^{n+\alpha} \quad (8b)$$

and where \mathbf{x}^{n+1^p} is a suitable predictor extrapolated from past solutions. The partitioning scheme is called implicit–implicit since all diagonal entries of \mathbf{B} remain on the left-hand side of (8), and both subsystems hence are approximated in an implicit way.

A wide variety of predictors can be selected based on multi-order multi-parameter numerical extrapolation techniques which may include derivatives of past solutions. The type of predictor invoked will likely influence the numerical stability of the partitioned solution procedure.¹⁶ One obvious form of the predictor is simply the solution at the previous time step. Park *et al.*¹⁷ demonstrated that this simple form is a stable predictor when used with a trapezoidal rule for fluid-structure interaction problems, while also remaining second-order accurate.

Using the solution at the previous time step as a simple predictor for the solution of (8), the partitioned solution procedure of the dual-porosity model proceeds now as follows.

- (i) Predict the pressure head field of one of the subsystems, e.g. the soil matrix subsystem, in eqn (8)

$$\mathbf{h}_m^{n+1^p} = \mathbf{h}_m^n \quad (9)$$

- (ii) Solve for the pressure head field of the fracture subsystem, i.e. \mathbf{h}_f in eqn (8a), using

$$\begin{aligned} [\mathbf{C}_f^{n+\alpha,i} + \alpha\Delta t(\mathbf{K}_f + \mathbf{E})^{n+\alpha,i}]\mathbf{h}_f^{n+1,i+1} &= \Delta t\mathbf{f}_f^{n+\alpha} \\ &+ [\mathbf{C}_f^{n+\alpha,i} - (1-\alpha)\Delta t(\mathbf{K}_f + \mathbf{E})^{n+\alpha,i}]\mathbf{h}_f^n \\ &+ (1-\alpha)\Delta t\mathbf{E}^{n+\alpha,i}\mathbf{h}_m^n + \alpha\Delta t\mathbf{E}^{n+\alpha,i}\mathbf{h}_m^{n+1^p} \end{aligned} \quad (10)$$

where the superscript i denotes the iteration level within the Picard iteration scheme.

- (iii) Correct the pressure head field in the matrix subsystem, i.e. \mathbf{h}_m in eqn (8a), as follows

$$\begin{aligned} [\mathbf{C}_m^{n+\alpha,i} + \alpha\Delta t(\mathbf{K}_m + \mathbf{E})^{n+\alpha,i}]\mathbf{h}_m^{n+1,i+1} &= \Delta t\mathbf{f}_m^{n+\alpha} \\ &+ [\mathbf{C}_m^{n+\alpha,i} - (1-\alpha)\Delta t(\mathbf{K}_m + \mathbf{E})^{n+\alpha,i}]\mathbf{h}_m^n \\ &+ (1-\alpha)\Delta t\mathbf{E}^{n+\alpha,i}\mathbf{h}_f^n + \alpha\Delta t\mathbf{E}^{n+\alpha,i}\mathbf{h}_f^{n+1} \end{aligned} \quad (11)$$

- (iv) The water flux field at time $n + 1$ can be calculated from the time rate of change of the water content $\dot{\theta}^{n+1}$, i.e.

$$\dot{\theta}_f^{n+1} = \mathbf{f}_f^{n+1} - (\mathbf{K}_f + \mathbf{E})^{n+1} \mathbf{h}_f^{n+1} + \mathbf{E}^{n+1} \mathbf{h}_m^{n+1} \quad (12a)$$

$$\dot{\theta}_m^{n+1} = \mathbf{f}_m^{n+1} - (\mathbf{K}_m + \mathbf{E})^{n+1} \mathbf{h}_m^{n+1} + \mathbf{E}^{n+1} \mathbf{h}_f^{n+1} \quad (12b)$$

or, alternatively, simply from Darcy's law using the solutions obtained from steps (ii) and (iii).

The above solution procedure is a single-pass solution scheme without iteration between the two subsystems. Steps (ii) and (iii) may be iterated, if desired, which leads to a predictor-independent stability condition identical to that of the simultaneous solution scheme provided that a sufficient number of iterations is carried out.¹⁶ Major concerns in practical applications of coupled field problems are the computational cost, numerical stability, and accuracy. Considerable effort has been devoted to searching for a stable single-pass partitioned scheme for coupled field problems.^{5,12,15,17,19,21} In the following sections we discuss the numerical stability and accuracy of the above solution scheme as applied to the dual-porosity flow problem.

The partitioned method results in a symmetric tridiagonal coefficient matrix of order N , where N is the number of degrees-of-freedom, for each subsystem. On the other hand, the simultaneous scheme leads to a symmetric seven-diagonal matrix of order $2N$. If a Cholesky decomposition method is used as the equation solver, the computational cost, evaluated in terms of the number of floating-point operations, is directly proportional to the order and the square of the upper (or lower) half-band width. Solving the coupled set of equations once with one Picard iteration requires approximately nine times more operations with the simultaneous scheme as compared with the partitioned scheme.

STABILITY ANALYSIS

The stability of an integration method depends on the eigenvalues of the approximation operator. One method^{14,16} of assessing numerical stability is to apply the solution amplification technique to the homogeneous time-discrete model eqn (8), and to search for nontrivial solutions of the form $\mathbf{x}^{n+1} = \gamma \mathbf{x}^n$, where γ is the solution amplification factor. The analysis was simplified by introducing the transformation¹⁴ $\gamma = (1+z)/(1-z)$ which maps the unit disc $|\gamma| \leq 1$ into the negative real half-plane $\text{Re}(z) \leq 0$, to which the Routh-Hurwitz stability criterion⁷ can be applied. Applying these procedures to eqn (8), and assuming a

free response of the system, leads to the following stability-governing characteristic polynomial for the single-pass partitioned integration scheme

$$\det \mathbf{J}(z) = 0 \quad (13a)$$

where

$$\mathbf{J}(z) = [2\mathbf{A}^{n+\alpha} + \alpha\Delta t(\mathbf{B}_1 - \mathbf{B}_E)^{n+\alpha} - (1-\alpha)\Delta t\mathbf{B}^{n+\alpha}]z + \Delta t\mathbf{B} \quad (13b)$$

Equation (13) can be reduced to a two-degree-of-freedom (2-dof) system of scalar equations by modal decomposition. The resulting scalar equation for nonlinear problems is also nonlinear.^{10,11} An essential property used in the reduction procedure is orthogonality of the eigenvectors of the associated eigenvalue problem

$$\Phi^T \mathbf{C} \Phi = \mathbf{I} \quad (14a)$$

$$\Phi^T (\mathbf{K} + \mathbf{E}) \Phi = \Lambda \quad (14b)$$

where \mathbf{I} is the identity matrix. The transformation matrix Φ is chosen such that the columns of Φ contain a complete set of orthogonal eigenvectors, whereas Λ is a diagonal matrix which stores the corresponding real and non-negative eigenvalues $\lambda_i(t)$ along its i th diagonal. The associated 2-dof scalar form of eqn (13) is

$$\det \begin{bmatrix} [2 + (2\alpha - 1)\Delta t\lambda_f]z + \Delta t\lambda_f & \Delta te z - \Delta te \\ (\Delta te - 2\alpha\Delta te)z - \Delta te & [2 + (2\alpha - 1)\Delta t\lambda_m]z + \Delta t\lambda_m \end{bmatrix} = 0 \quad (15)$$

in which e represents a generalized physical quantity corresponding to the exchange term. The value e is real and non-negative. Note that λ_f , λ_m , and e are all functions of the corresponding generalized dependent variables, and hence are functions of time. Since these three quantities are evaluated at time $(n+\alpha)\Delta t$ (i.e. $\lambda_f^{n+\alpha}$, $\lambda_m^{n+\alpha}$ and $e^{n+\alpha}$), the superscripts $n+\alpha$ in eqn (15) and all following equations are eliminated to simplify the notation. Expanding (15) yields

$$a_0 z^2 + a_1 z + a_2 = 0 \quad (16a)$$

where

$$\begin{aligned} a_0 &= [2 + (2\alpha - 1)\Delta t\lambda_f][2 + (2\alpha - 1)\Delta t\lambda_m] \\ &\quad + (2\alpha - 1)\Delta t^2 e^2 \\ a_1 &= [2 + (2\alpha - 1)\Delta t\lambda_f]\Delta t\lambda_m \\ &\quad + [2 + (2\alpha - 1)\Delta t\lambda_m]\Delta t\lambda_f + 2(1 - \alpha)\Delta t^2 e^2 \\ a_2 &= \Delta t^2 \lambda_f \lambda_m - \Delta t^2 e^2 \end{aligned} \quad (16b)$$

According to the Routh-Hurwitz criterion, the characteristic polynomial (16) has a zero or negative real part if and only if $a_0 > 0$, and a_1 and $a_2 \geq 0$.⁷ The condition $\alpha \geq 1/2$ implies that both a_0 and a_1 are

positive, while the condition $\lambda_f \lambda_m \geq e^2$ must be satisfied in order for $a_2 \geq 0$ to be valid. One may show that the inequality $(\mathbf{K}_f + \mathbf{E})(\mathbf{K}_m + \mathbf{E}) \geq \mathbf{E}^2$ in matrix form always holds, and from this it follows that the requirement $a_2 \geq 0$ is satisfied automatically. The single-pass partitioned scheme (eqns (9)–(11)) is thus unconditionally stable for $\alpha \geq 1/2$.

For $0 \leq \alpha < 1/2$, the following two restrictions, posed by $a_0 > 0$ and $a_1 \geq 0$, have to be satisfied simultaneously

$$4 + (1 - 2\alpha)^2 \Delta t^2 \lambda_f \lambda_m > (1 - 2\alpha) \times [2\Delta \lambda_m + 2\Delta t \lambda_f + \Delta t^2 e^2] \quad (17a)$$

$$2\Delta t \lambda_m + 2\Delta t \lambda_f + 2(1 - \alpha) \Delta t^2 e^2 \geq 2(1 - 2\alpha) \Delta t^2 \lambda_f \lambda_m \quad (17b)$$

Substituting (17b) into (17a) and rearranging leads to a restriction for the step size in the time domain

$$\Delta t^2 < \frac{4}{(1 - 2\alpha)^2 (\lambda_f \lambda_m - e^2)} \quad (18)$$

Hence the partitioned solution scheme is only conditionally stable when $0 \leq \alpha < 1/2$.

If there is no exchange term, the dual-porosity model would result in two independent Richards equations which could be solved sequentially using the same time step Δt . Equation (18) becomes then

$$\Delta t^2 < \frac{4}{(1 - 2\alpha)^2 \bar{\lambda}_f \bar{\lambda}_m} \quad (19)$$

where $\bar{\lambda}$ is a generalized physical quantity corresponding to the conductivity matrix \mathbf{K} . Equation (19) specifies that the time step has to be chosen as a minimum of the two restrictions

$$\Delta t < \min \left[\frac{2}{(1 - 2\alpha) \bar{\lambda}_f}, \frac{2}{(1 - 2\alpha) \bar{\lambda}_m} \right] \quad (20)$$

If we further assume that the two subsystems have identical soil-hydraulic properties, eqn (19) reduces to

$$\Delta t < \frac{2}{(1 - 2\alpha) \bar{\lambda}} \quad (21)$$

which is identical to the stability requirement for linear parabolic problems as discussed in some standard textbooks (e.g. the book of Burnett³). Note that the stability restriction for nonlinear equations has the same form as that of linear problems when integrated by the

midpoint rule^{10,11} except that $\bar{\lambda}$ in (21) is now a function of time.

ACCURACY ANALYSIS

Expanding the exact solutions of h_f^{n+1} , h_f^n , h_m^{n+1} , and h_m^n about time $(n + \alpha)\Delta t$ by means of finite Taylor expansions, and substituting the resulting expressions into eqn (8) leads to

$$\begin{aligned} & \mathbf{C}_f^{n+\alpha} \mathbf{h}_f^{n+\alpha} + (\mathbf{K}_f + \mathbf{E})^{n+\alpha} \mathbf{h}_f^{n+\alpha} - \mathbf{E}^{n+\alpha} \mathbf{h}_m^{n+\alpha} \\ & = \mathbf{f}_f^{n+\alpha} + (1 - 2\alpha)O(\Delta t) + O(\Delta t^2) \\ & \mathbf{C}_m^{n+\alpha} \mathbf{h}_m^{n+\alpha} + (\mathbf{K}_m + \mathbf{E})^{n+\alpha} \mathbf{h}_m^{n+\alpha} - \mathbf{E}^{n+\alpha} \mathbf{h}_f^{n+\alpha} \\ & = \mathbf{f}_m^{n+\alpha} + (1 - 2\alpha)O(\Delta t) + O(\Delta t^2) \end{aligned} \quad (22)$$

Comparing eqn (22) with eqn (5), evaluated at time $n + \alpha$, it can be shown that the local truncation errors T for both subsystems are of the form

$$T = (1 - 2\alpha)O(\Delta t) + O(\Delta t^2) \quad (23)$$

Thus the numerical solutions are second-order accurate when the midpoint rule ($\alpha = 1/2$) is used.

SIMULATION EXAMPLES

Two simulation examples, each involving three different water exchange rates Γ_w , will be presented to show the accuracy and stability of the proposed single-pass partitioned solution procedure. To facilitate comparison with previous solutions, we assumed the same hydraulic properties of the physical system as those employed by Gerke and van Genuchten⁸ (Table 1). For the first example, we further assumed similar initial and surface boundary conditions as invoked by Gerke and van Genuchten.⁸ The example considers a 40-cm-deep soil column initially at a uniform pressure head of -1000 cm and subjected to a constant infiltration rate of 1000 cm day⁻¹ applied to the fracture pore domain. The lower boundaries of both subsystems were assumed to be free drainage conditions (i.e. $\partial h / \partial z = 0$). Parameters defining the water transfer coefficient α_w in eqn (3) were chosen to be $\beta = 0.3$, $\gamma_w = 0.4$, $K_a = 0.5[K_a(h_f) + K_a(h_m)]$, whereas the matrix block size, a , was left variable for different simulation scenarios.

Figure 1 shows the simulation results for three different rates of water exchange between the two pore

Table 1. Hydraulic parameters used in the simulations

| | θ_r | θ_s | α (cm ⁻¹) | n | K_y (cm day ⁻¹) | ϵ |
|---------------|------------|------------|------------------------------|-----|-------------------------------|------------|
| Matrix | 0.10526 | 0.5 | 0.005 | 1.5 | 1.0526 | 0.95 |
| Fracture | 0.0 | 0.5 | 0.1 | 2.0 | 2000.0 | 0.05 |
| Exchange term | 0.10526 | 0.5 | 0.005 | 1.5 | 0.01 | — |

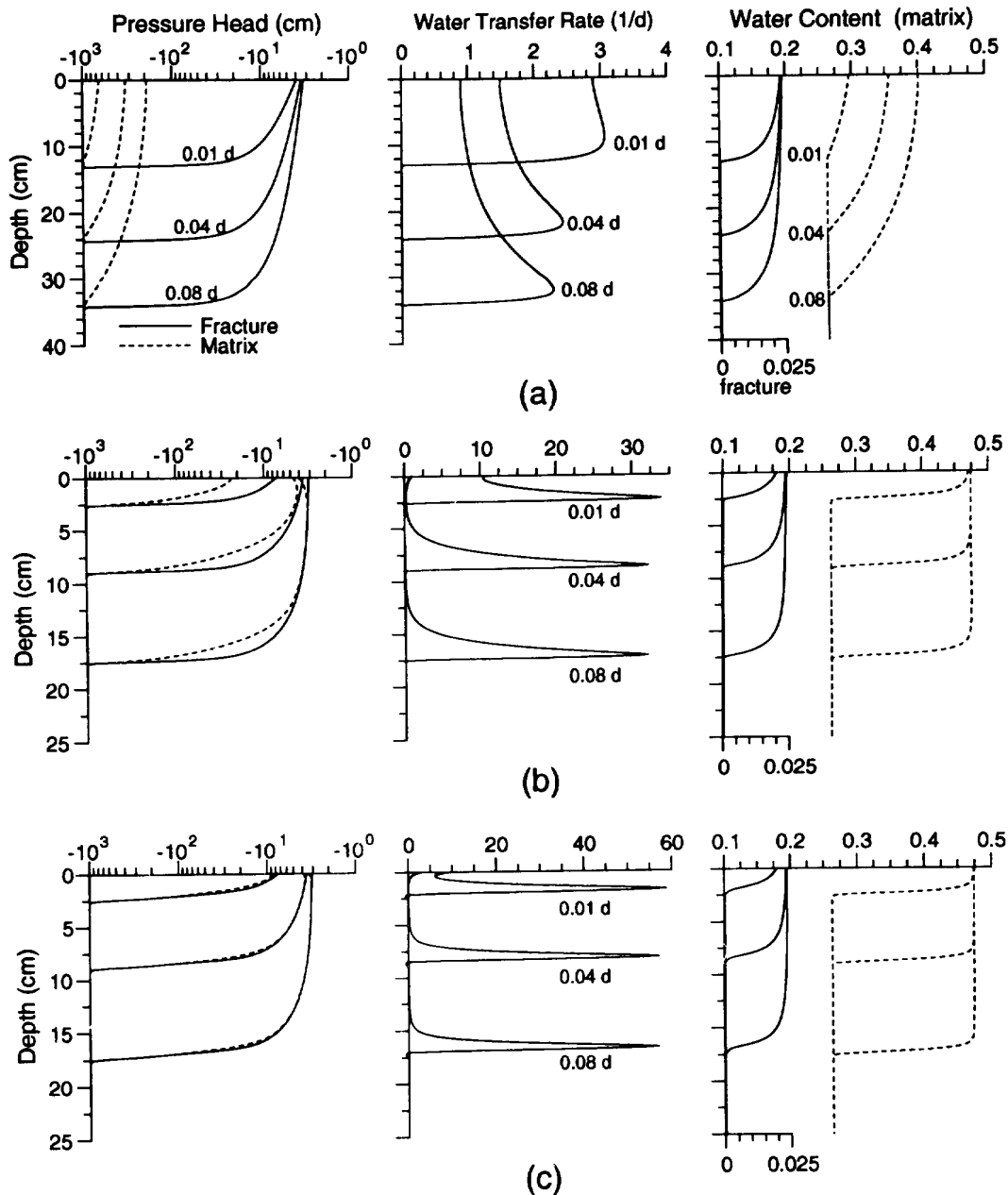


Fig. 1. Distribution of the pressure head, water transfer rate, and volumetric water content at selected times for three different values of water transfer coefficient caused by changes in the characteristic length of the matrix blocks: (a) $a = 1$ cm, (b) $a = 0.1$ cm, and (c) $a = 0.0316$ cm. Note the different scales used in the plots for the volumetric water content.

domains. The first case (Fig. 1(a)) assumed the same exchange term as used by Gerke and van Genuchten⁸ ($a = 1$ cm). The other two cases were simulated by decreasing the value of a such that the mass transfer rate, α_w , increased by factors of 100, and 1000 times. As expected, and shown by the results in Figs 1(b) and 1(c), the two subsystems gradually approach an instantaneous equilibrium situation in which the two subsystems attain the same distributions of h versus depth. The positive pressure gradient found in the region

immediately below the soil surface in the matrix subsystem is caused by a combination of the lateral flux from exchange and the downward moving Darcian flux, while no water is allowed to enter the surface of the matrix subsystem. The same phenomenon was also observed when using the simultaneous solution scheme.⁸

The three cases in Fig. 1 were simulated using the single-phase scheme, as well as a scheme which employs iteration between the two subsystems. The computational

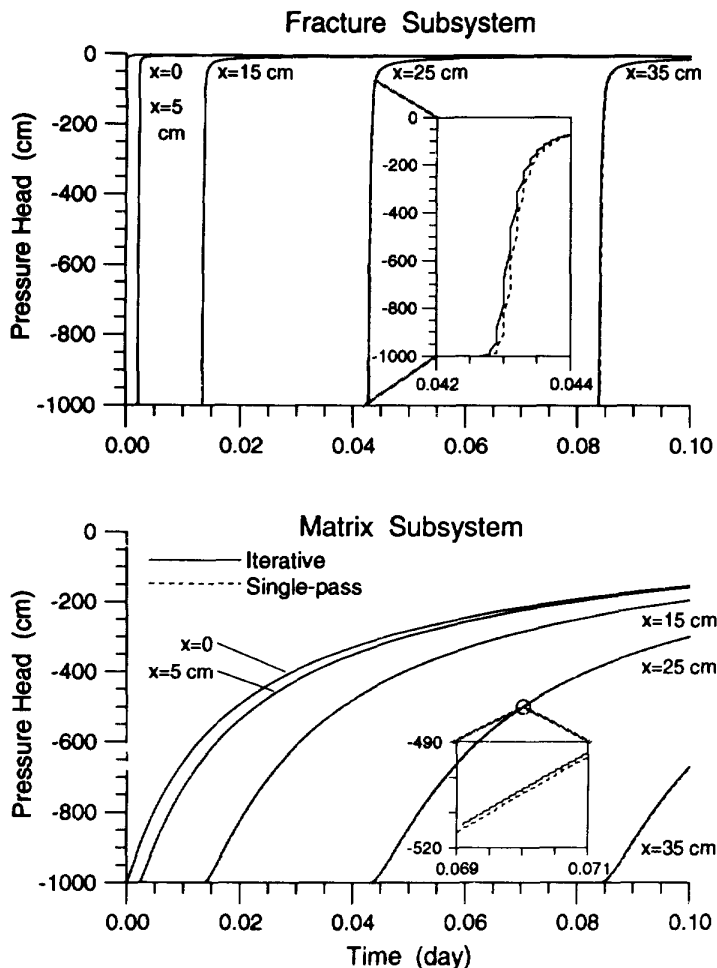


Fig. 2. Evolution of pressure head versus time at selected depths in both subsystems as calculated by the single-pass and iterative schemes assuming a characteristic half-width of the matrix block of 1 cm.

efficiency was enhanced by employing in the calculation an adaptive time-step so as to optimize the time-step and minimize the number of Picard iterations when solving the equation of each subsystem. The results obtained with both schemes were found to be indistinguishable when plotted in the figure. The results for the case where $a = 1$ cm (Fig. 1(a)) show excellent agreement with results obtained by Gerke and van Genuchten⁸ using a simultaneous solution scheme. This duplication of results verifies that the single-pass partitioned solution procedure is stable for the wide range of water exchange rates tested provided that the integration is carried out with $\alpha \geq 1/2$ in time.

Additional comparisons of the single-pass and iterative solution results are depicted in Fig. 2. This figure shows pressure head changes in both subsystems at five selected depths, plotted as a function of time for the case where $a = 1$ cm. The enlarged windows in Fig. 2 show the type of deviations obtained between the two numerical schemes. Assuming that the iterative scheme

likely approximated the exact solution somewhat better, the single-pass scheme hence caused a slightly delayed response of the system due to extrapolation of the coupling term from solutions at the previous time step. The magnitude of this delay is proportional to the value of the water exchange rate. Fortunately, the delay effect can be made negligibly small, even for cases having extreme water transfer rates, by reducing the size of the time step. Cutting the time step-size with a single-pass scheme is usually more effective than prolonged iteration between the two subsystems.⁶ The cost of reducing the time step-size for highly nonlinear systems is generally compensated by a reduced number of Picard iterations required for solving each subsystem. Moreover, one may argue that the limiting case of instantaneous or nearly-instantaneous equilibrium is of little practical interest, since such a case is better simulated with the standard one-equation Richards model using appropriate field hydraulic properties. The three simulation cases illustrated in this example pertained to characteristic

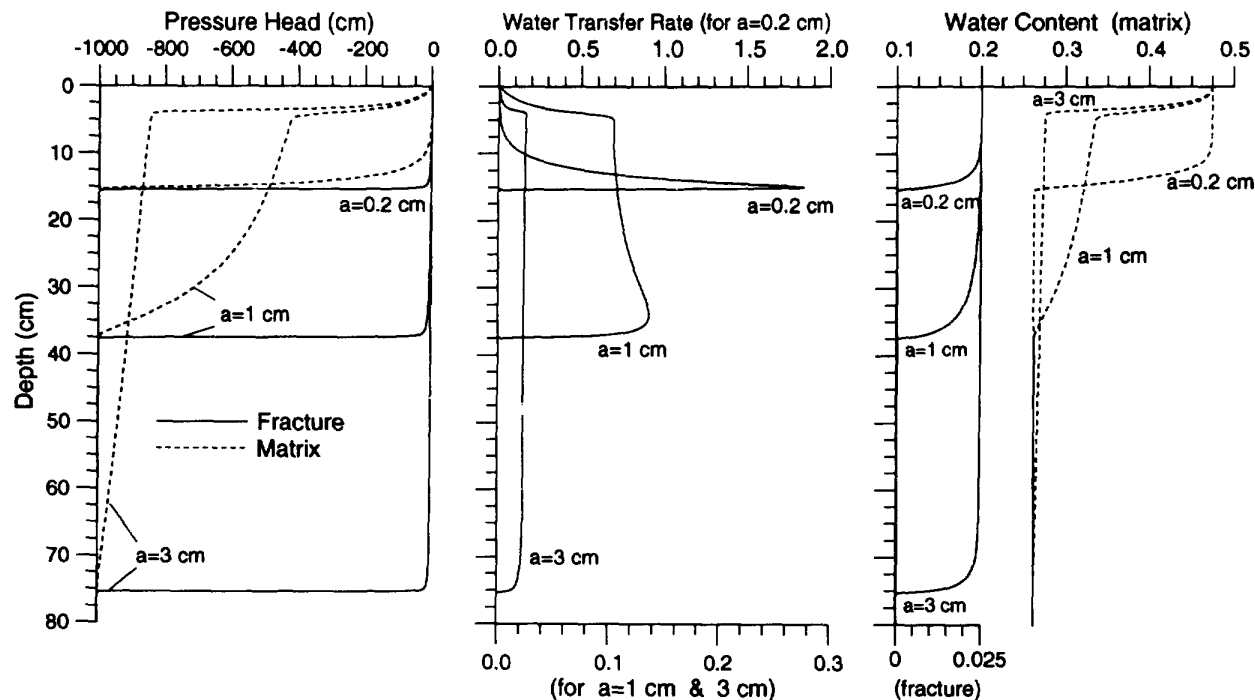


Fig. 3. Distributions of the pressure head, water transfer rate, and volumetric water content after 0.5-h of ponding. Note the different scales used in the plot for the corresponding curves of the water transfer rate and water content.

half-widths, a , of the matrix block of 1, 0.1, and 0.0316 cm, respectively.

The second example simulates ponded irrigation of water into an 80-cm deep, initially dry dual-porosity medium. The same hydraulic properties as for the previous example were used (Table 1). We also used the same parameters for the water transfer coefficient, except for the matrix block size a which was assumed to be 0.2, 1, and 3 cm, respectively, for three different test cases. A prescribed pressure head of 0.3 cm was imposed at the soil surface, whereas an initially uniform pressure head of -1000 cm was assumed for both subsystems. The lower boundary again was assumed to be a free drainage surface.

Figure 3 depicts the simulation results for three different water transfer rates after 0.5 h of ponding. Nearly identical results were obtained when simulated with the same time step size using both the single-pass and iterative schemes. Preferential movement of water in the fracture subsystem can be very significant when the water transfer rate is relatively small (i.e. $a = 3$ cm). The shape of the pressure head profile in the matrix zone shows an abrupt change in gradient, a feature which can be used to distinguish the contribution from either ponded infiltration or lateral exchange. On the other hand, when the exchange rate dominates (i.e. $a = 0.2$ cm), preferential flow in the fracture zone is diminished and surface infiltration of water into the matrix zone is embedded in the moisture front.

CONCLUSIONS

A partitioned solution procedure, previously developed for solving problems of coupled mechanical systems, was applied to the solution of the coupled equations of water flow in a variably saturated dual-porosity medium. The solution method is shown to be stable and second-order accurate when integrated by a midpoint rule in time, even when only a single-pass through the partitioned equations is made during each time step. The proposed single-pass scheme is shown to be computationally much more efficient than simultaneous solution methods, and hence more suitable for practical applications.

REFERENCES

1. Barenblatt, G. I. & Zheltov, I. P., Fundamental equations of filtration of homogeneous liquids in fissured rocks. *Dokl. Akad. Nauk. SSSR*, **13** (1960) 545–8.
2. Barenblatt, G. I., Zheltov, I. P. & Kochina, I. N., Basic concepts in the theory of seepage of homogeneous liquids in fissured rocks. *J. Appl. Math. Mech.* (Engl. Transl.) **24** (1960) 1286–1303.
3. Burnett, D. S., *Finite Element Analysis: From Concepts to Applications*. Addison-Wesley Publ. Co., Reading, MA, USA, 1987.
4. Celia, M. A., Bouloutas, E. T. & Zhabba, R. L., A general mass-conservative numerical solution for the unsaturated flow equation. *Water Resour. Res.*, **26** (1990) 1483–96.
5. Farhat, C., Park, K. C. & Dubois-Pelerin, Y., An unconditionally stable staggered algorithm for transient

- finite element analysis of coupled thermoelastic problems. *Comp. Meths Appl. Mech. Engng*, **85** (1991) 349–65.
6. Felippa, C. A. & Park, K. C., Staggered transient analysis procedures for coupled mechanical systems: formulation. *Comp. Meths Appl. Mech. Engng*, **24** (1980) 61–111.
 7. Gantmacher, F. R., *The Theory of Matrices, Vol. 2*. Chelsea Publ. Co., New York, USA, 1959.
 8. Gerke, H. H. & van Genuchten, M. T., A dual-porosity model for simulating the preferential movement of water and solutes in structured porous media. *Water Resour. Res.*, **29** (1993) 305–19.
 9. Gerke, H. H. & van Genuchten, M. T., Evaluation of a first-order water transfer term for variably saturated dual-porosity flow models. *Water Resour. Res.*, **29** (1993) 1225–38.
 10. Gourlay, A. R., A note on trapezoidal methods for the solution of initial value problems. *Maths Comp.*, **24** (1970) 629–33.
 11. Hughes, T. J. R., Unconditionally stable algorithms for nonlinear heat conduction. *Comp. Meths Appl. Mech. Engng*, **10** (1977) 135–9.
 12. Li, X., Finite-element analysis for immiscible two-phase fluid flow in deforming porous media and an unconditionally stable staggered solution. *Commun. Appl. Numer. Meths*, **6** (1990) 125–35.
 13. Mills, W. B., Johns, R. A. & White, C., *Review and Evaluation of Approaches to Simulate Flow and Solute Transport Through Macroporous Media*. Tetra Tech, Inc., Lafayette, California, USA, 1991.
 14. Park, K. C., Partitioned transient analysis procedures for coupled-field problems: stability analysis. *J. Appl. Mech.*, **47** (1980) 370–6.
 15. Park, K. C., Stabilization of partitioned solution procedures for pore fluid–soil interaction analysis. *Int. J. Numer. Meths Engng*, **19** (1983) 1669–73.
 16. Park, K. C. & Felippa, C. A., Partitioned analysis of coupled systems. In *Computational Methods for Transient Analysis*, eds T. Belytschko & T. J. R. Hughes, Elsevier Sci. Pub., Amsterdam, The Netherlands, 1983, pp. 157–219.
 17. Park, K. C., Felippa, C. A. & DeRuntz, J. A., Stabilization of staggered solution procedures for fluid–structure interaction analysis. In *Computational Methods for Fluid–Structure Interaction Problems*, eds T. Belytschko & T. L. Geers. ASME Applied Mechanics Symposia Series, AMD-Vol. 26, 1977, pp. 94–124.
 18. Rathfelder, K. & Abriola, L. M., Mass conservative numerical solutions of the head-based Richards equation. *Water Resour. Res.*, **30** (1994) 2579–86.
 19. Simoni, L. & Schrefler, B. A., A staggered finite-element solution for water and gas flow in deforming porous media. *Commun. Appl. Numer. Meths*, **7** (1991) 213–223.
 20. van Genuchten, M. T., A closed-form equation for predicting the hydraulic conductivity of unsaturated soils. *Soil Sci. Soc. Am. J.*, **44** (1980) 892–8.
 21. Zienkiewicz, O. C., Paul, D. K. & Chan, A. H. C., Unconditionally stable staggered solution procedure for soil–pore fluid interaction problems. *Int. J. Numer. Meths Engng*, **26** (1988) 1039–55.

APPENDIX

Expressions for matrices in eqn (5), as given below, are similar for both subsystems. The subscripts f (fractures) and m (matrix blocks) hence can be added accordingly to the following equations to represent the expressions for the two subsystems.

$$\mathbf{C} = \sum_e \epsilon \int_{L_e} C_j N_i N_j dx \quad (\text{A1})$$

$$\mathbf{K} = \sum_e \epsilon \int_{L_e} \hat{K} \frac{\partial N_i}{\partial x} \frac{\partial N_j}{\partial x} dx \quad (\text{A2})$$

$$\mathbf{E} = \sum_e \alpha_w^* \int_{L_e} \hat{K}_a N_i N_j dx \quad (\text{A3})$$

$$\mathbf{f} = \sum_e \epsilon \int_{L_e} \cos \alpha \hat{K} \frac{\partial N_i}{\partial x} dx - \sum_e \epsilon \int_{L_e} \hat{S} N_i dx + \sum_e \epsilon N_i K \left(\frac{\partial h}{\partial x} - \cos \alpha \right) \Big|_{L_e} \quad (\text{A4})$$

where N_i are the weighing functions which in the Galerkin approach are identical to the basis functions N_j , L_e is the length of the element e , α_w^* is defined as $\beta \gamma_w / a^2$, and \hat{K} , \hat{K}_a , and \hat{S} are the expansions of the corresponding variable parameters within an element in terms of the basis functions. Note that the capacity coefficients C are evaluated with the standard chord-slope approximation to achieve reliable mass balance accuracy.¹⁸